行政院國家科學委員會專題研究計畫　期中進度報告

多埠微波網路量測技術之建立及應用(2/3)

計畫類別：個別型計畫
計畫編號：NSC93-2213-E-002-035-
執行期間：93 年 08 月 01 日至 94 年 07 月 31 日
執行單位：國立臺灣大學電信工程學研究所

計畫主持人：瞿大雄

報告類型：精簡報告

處理方式：本計畫可公開查詢

中　華　民　國 94 年 5 月 31 日

行政院國家委員會專題研究計畫期中進度報告

多埠微波網路量測技術之建立及應用(2/3)

Development and application of multiport microwave network measurement techniques (2/3)

計畫編號：NSC93-2213-E-002-035
執行期限：93年8月1日至94年7月31日
計畫主持人：瞿大雄 教授 國立台灣大學電信工程學研究所

一、 中文摘要

本計畫為一三年計畫(92年至95年)，進行「多埠微波網路量測技術之建立及應用」研發工作。本報告係敘述第二年之研究成果，主要係建立「多埠激發法」於微波影像之應用，共建立三項使用多源照射之新型掃描微波影像技術，包含準單向式、雙向式及多向式配置。分別敘述其原理、量測系統、校準公式及量測結果。由實驗結果顯示，所研製之三項微波成像系統，相對於傳統單源照射之微波成像量測系統，可改善其影像解析度、散射物體之視角及擷取傳氏空間資料之效率。

關鍵詞：多埠激發−多埠接收法、微波影像。

英文摘要

This is a three-year project (from 92/8 to 95/7) to conduct researches on multiport microwave network measurement techniques. In this second-year report, the study results are mainly focused on the development of microwave diversity imaging of conducting objects using multi-source illumination. Three frequency-swept microwave imaging arrangements, namely quasi-monostatic, bistatic and multistatic arrangements, using multi-source illumination technique are developed. These three arrangements are shown experimentally that the multi-source illumination is an effective approach to yield good image resolution and viewing angle of conducting object by effectively extending the recorded scattering information in the Fourier domain.

Keywords: multiport-stimulas and multiport-receiving method, microwave imaging.

二、 計畫緣由與目的

Microwave imaging is an approach to reconstruct the scattering object characteristics from the recorded object scattered field in the microwave frequency range. For the microwave imaging of conducting objects, frequency and angular diversity techniques are applied in the quasi-monostatic and bistatic arrangements using single source illumination [1, 2].

In this report, we present the second-year research results [3-5] on the development of three swept-frequency microwave imaging systems using multi-source illumination technique. The reconstructed image gives an image corresponding to the induced surface current distribution on the illuminated region due to the specular diffraction observed by receiving antennas. Since the scattering object is illuminated by multi-sources, the induced current contributed from each illuminating source then interferes with others on the object surface. The recorded object scattered field is therefore a coherent summation of the scattered fields from the illuminated regions. In this study, image reconstruction methods are developed to use sets of equations in the Fourier-domain to solve the corresponding portion of scattered field contributed from each illumination source. As the results, the multi-source illumination technique will enlarge the illuminated region on the scattering object surface hence to improve the resulting image viewing angle and resolution.

三、 研究方法及成果

I. Quasi-monostatic Arrangement

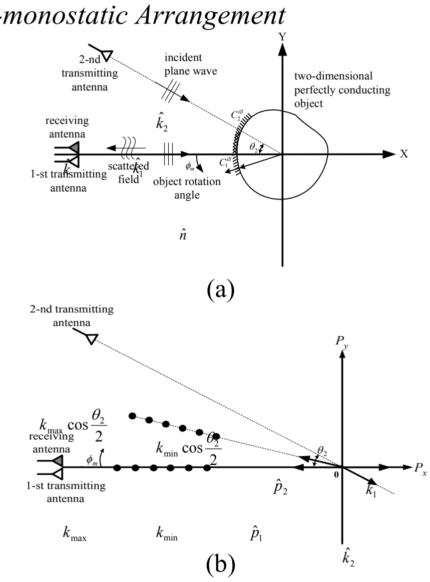

Fig. 1 (a) Quasi-monostatic arrangement with two-source illumination and (b) its frequency-swept Fourier domain.

Figure 1 shows the quasi-monostatic backscattering geometry for multi-source illumination. The scattering object is illuminated by multiple normally incident TM-polarized plane waves simultaneously. The transmitting and receiving antennas are in the far-field region. The scattered field recorded by the receiving antenna can be represented as

$$U^s = \frac{-jk_0 e^{-jkr}}{|\bar{r}-\bar{r}'|}\sum_{i=1}^{n} E_i \iint O_i(\bar{r}') e^{jk_0(\hat{k}-\hat{k}_i)\cdot\bar{r}'} d^2\bar{r}' \qquad (1)$$

where E_i is the amplitude of the *i*-th illuminating plane wave. $O_i(\bar{r}')$ is the partial microwave image contributed from the *i*-th source illumination.

By performing the Fourier transformation, (1) can be expressed as

$$U^s = C_R \sum_{i=1}^{n} E_i \widetilde{O}_i(\bar{p}_i) \qquad (2)$$

where C_R is the range related term $-jk_0 e^{-jkr}/|\bar{r}-\bar{r}'|$. $\bar{p}_i$ is defined as

$$\bar{p}_i = p_i \hat{p}_i = k_0(\hat{k}-\hat{k}_i) = k_0 \cos\frac{\theta_i}{2}\hat{p}_i \qquad (3)$$

where θ_i is the angle between *i*-th source and the receiving antenna. The Fourier transformation of $O_i(\bar{r})$ is given as

$$\widetilde{O}_i(\bar{p}_i) = \iint O_i(\bar{r}) e^{j\bar{p}_i\cdot\bar{r}} d^2\bar{r}\ . \qquad (4)$$

In order to properly extract each partial microwave image contributed from the corresponding source illumination, a set of n arrangements of (2) with different illuminating amplitude E_i are written as

$$\begin{bmatrix} U_1^s \\ U_2^s \\ \vdots \\ U_n^s \end{bmatrix} = C_R \begin{bmatrix} E_{11} & E_{12} & \cdots & E_{1n} \\ E_{21} & E_{22} & \cdots & E_{2n} \\ \vdots & \vdots & \ddots & \vdots \\ E_{n1} & E_{n2} & \cdots & E_{nn} \end{bmatrix} \begin{bmatrix} \widetilde{O}_1 \\ \widetilde{O}_2 \\ \vdots \\ \widetilde{O}_n \end{bmatrix}. \qquad (5)$$

With the use of frequency diversity technique to have k_0 swept from k_1 to k_2, (5) shows that *n* lines of the Fourier-domain data contributed from *n* illumination sources can be extracted from the *n* sets of scattered field recorded at one viewing angle, as the matrix $[E_{ij}]$ is a known non-singular matrix. In other words, an *n*-fold Fourier-domain data can be obtained by using *n*-source illumination. This is then equivalent to the Fourier-domain data obtained with single-source illumination at *n* different object rotation angles. Therefore, by correctly locating the exacted Fourier-domain data one can effectively acquire the object Fourier-domain information. Figure 1(b) shows the two-line Fourier-domain data acquired using two-source illumination.

A quasi-monostatic microwave imaging system is developed wth three horn antennas at about $30°$, $0°$ and $-30°$ for simultaneously transmitting frequency-swept microwave signals with power levels controlled by three attenuators. The receiving horn antenna is at about 0° for collecting the object scattered field. An Agilent 8722ES network analyzer is used to measure the object scattered field. In the measurement, the frequency is stepped from 7.5 to 12.5 GHz for 51 points and object scattered field is recorded at a total of 120 viewing angles with 1° interval. This then gives a total of 360° spanned Fourier-domain data. Therefore, it effectively reduces the object rotation angle by three times. The scattering object is a metallic cylinder with 15 cm radius. Figure 2 shows the measured Fourier-domain data and the reconstructed image. The experimental results are shown in good agreement with the scattering object geometry.

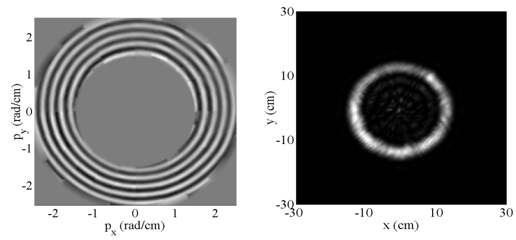

(a) (b)

Fig. 2 (a) Measured Fourier-domain data and (b) reconstructed image using quasi-monostatic arrangement.

B. Bistatic Arrangement

The scattering geometry of bistatic scattering arrangement is shown in Fig. 3. The scattering object is illuminated by multiple normally incident TM-polarized plane waves simultaneously as in Fig. 1(a). However, the scattering information is recorded by a backward linear receiving array at $z=-d$ in this arrangement and can be represented as

$$U^s(x, z=-d, k_0) = \kappa \sum_{i=1}^{n} E_i \iint O_i(\bar{r}') e^{-jk_0\hat{k}_i\cdot\bar{r}'} G(|\bar{r}-\bar{r}'|) d^2\bar{r}' \qquad (6)$$

where $\kappa = -jk_0$. E_i and $O_i(\bar{r}')$ are defined in (1).

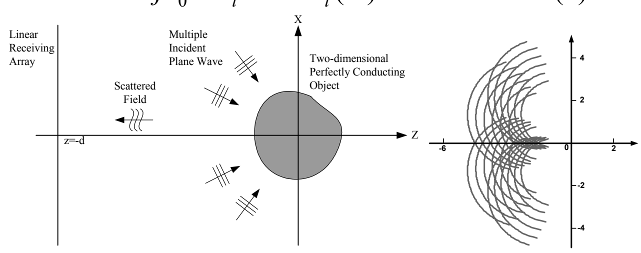

(a) (b)

Fig. 3 (a) Bistatic arrangement with four-source illumination and (b) its frequency-swept Fourier domain.

By using plane wave expansion of the Green's function, the Fourier transformation of (6) can be expressed as

$$\widetilde{U}^s(k_x, z=-d, k_0) = \frac{-j\kappa}{2\gamma} e^{-j\gamma d}\sum_{i=1}^{n} E_i \widetilde{O}_i(k_x,-\gamma,-k_0) \qquad (7)$$

where the Fourier transformation of $U^s(x, z=-d, k_0)$ is defined as

$$\widetilde{U}^s(k_x, z=-d, k_0) = \int U^s(x, z=-d, k_0) e^{jk_x x} dx . \qquad (8)$$

Similar to the quasi-monostatic arrangement, in order to properly extract each partial microwave image contributed from the corresponding source illumination, a set of n arrangements of (7) with different illuminating amplitude E_i are written as

$$\begin{bmatrix} \widetilde{U}_1^s(k_x,z=-d,k_0) \\ \widetilde{U}_2^s(k_x,z=-d,k_0) \\ \vdots \\ \widetilde{U}_n^s(k_x,z=-d,k_0) \end{bmatrix} = \frac{j2\gamma}{\kappa} e^{j\gamma d} \begin{bmatrix} E_{11} & E_{12} & \cdots & E_{1n} \\ E_{21} & E_{22} & \cdots & E_{2n} \\ \vdots & \vdots & \ddots & \vdots \\ E_{n1} & E_{n2} & \cdots & E_{nn} \end{bmatrix} \begin{bmatrix} \widetilde{O}_1(k_x,-\gamma,-k_0) \\ \widetilde{O}_2(k_x,-\gamma,-k_0) \\ \vdots \\ \widetilde{O}_n(k_x,-\gamma,-k_0) \end{bmatrix} \qquad (9)$$

Each partial microwave image data can then be extracted from the scattering data in the Fourier-space as the matrix $[E_{ij}]$ is non-singular. Therefore, by combining partial image data in the Fourier space, microwave image with a higher resolution and wider viewing angle can be achieved by taking a two-dimensional inverse Fourier transformation.

A bistatic microwave imaging system is developed with four horn antennas at about $\pm 30°$ and $\pm 60°$ for simultaneously transmitting frequency-swept microwave signals with power levels controlled by four attenuators. An open-ended WR-90 waveguide is used as a receiving probe, located on a 158 cm long linear scanner at about $z=-100$ cm for collecting the object scattered field. In the measurement, the frequency is stepped from 7.5 to 12.5 GHz for 51 points and a total of 128 positions are scanned along the linear scanner.

Figure 4 shows the measured Fourier-space data and reconstructed image of a metallic cylinder. The reconstructed image shows an about 60° circular ring image corresponding to the shape of the metallic cylinder.

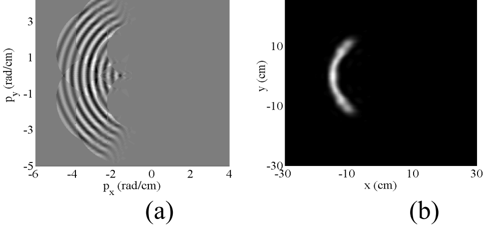

(a) (b)

Fig. 4 (a) Measured Fourier-domain data and (b) reconstructed image using bistatic arrangement.

C. Multistatic Arrangement

Figure 5(a) shows the scattering geometry of multistatic arrangement. With the use of frequency-swept technique, each pair of source and receiver can yield a line of Fourier-domain data. As shown in Fig. 5 (b), a two-source and two-receiver multistatic arrangement can give a total of four lines of Fourier-domain data. Whereas the quasi-monostatic arrangement shown in Fig. 1 (a), two-source and one-receiver can only give two lines of Fourier-domain data as shown in Fig. 1 (b). Therefore, one can effectively increase the number of lines of Fourier-domain data by using the multistatic arrangement. In addition, the multistatic arrangement is shown to give a wider object viewing angle.

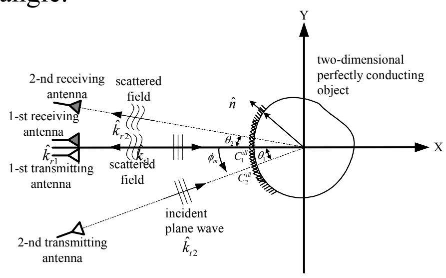

(a)

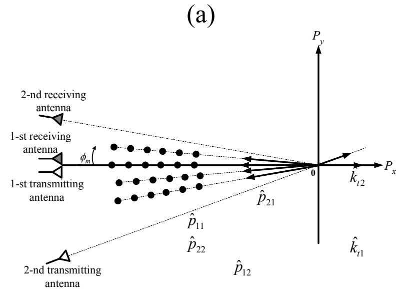

(b)

Fig. 5 (a) Multistatic arrangement with two-source illumination and (b) its frequency-swept Fourier domain.

Based on (1), the incident field for two-source illumination can be written as

$$\bar{E}^i(\bar r) = \hat z E_1 e^{-jk_0\hat k_{t1}\cdot\bar r} + \hat z E_2 e^{-jk_0\hat k_{t2}\cdot\bar r} = \sum_{j=1}^{2} \hat z E_j e^{-jk_0\hat k_{tj}\cdot\bar r} \qquad (10)$$

where $\hat k_{tj}$ is the direction of the j-th incident plane wave and E_j is the complex field of the j-th incident plane wave. The scattered fields contributed from two sources at two receiving antennas are given as

$$\bar E^s = -jk_0\sum_{j=1}^{2}\int_{C_j^{ill}} 2\hat n(\bar r')\times(\hat k_{tj}\times\hat z)E_j e^{-jk_0\hat k_{tj}\cdot\bar r'} G(|\bar r_i - \bar r'|)d\bar r' \quad i=1,\ 2 \qquad (11)$$

where C_j^{ill} is the illuminated object contour contributed from the j-th source, $\bar k_{ri} = k_0\hat k_{ri}$ and $\hat k_{ri}$ is the direction of each receiving antenna.

As the polarizations of two receiving antennas are in the z-direction, from (10) and (11), the scattered field in the far-field region becomes

$$U_i^s \approx \frac{-jk_0 e^{-jk_0 r_i}}{r_i} \sum_{j=1}^{2} E_j \iint O_{ij}(\bar{r}') e^{-jk_0(\hat{k}_{ri}-\hat{k}_{tj})\cdot\bar{r}'} d^2\bar{r}' \quad i=1,\ 2 \qquad (12)$$

where $O_{ij}(\bar{r}') = 2\hat{n}(\bar{r}')\cdot\hat{p}_{ij}\delta(C_j(\bar{r}'))$ is defined as the partial object function contributed from the *i*-th receiver and the *j*-th source. $\hat{p}_{ij}$ is the unit wave vector defined as $\hat{p}_{ij} = (\hat{k}_{ri}-\hat{k}_{tj})\,|\,\hat{k}_{ri}-\hat{k}_{tj}\,|$. $\delta(C_j(\bar{r}'))$ is an one-dimensional Dirac delta function corresponding to the *j*-th source. By defining the Fourier transformation of $O_{ij}(\bar{r}')$ as

$$\widetilde{O}_{ij}(\bar{p}_{ij}) = \iint O_{ij}(\bar{r}') e^{j\bar{p}_{ij}\cdot\bar{r}} d^2\bar{r}, \qquad (13)$$

(12) can be expressed as

$$U_i^s = C_R \sum_{j=1}^{2} E_j \widetilde{O}_{ij}(\bar{p}_{ij}) \quad i=1,\ 2 \qquad (14)$$

where C_R is the range related term $-jk_0 e^{-jk_0 r_i}/r_i$, and

$$\bar{p}_{ij} = k_0 \cos\frac{\varphi_{ij}}{2}(\sin\phi_m \hat{p}_x + \cos\phi_m \hat{p}_y)\,. \qquad (15)$$

φ_{ij} is the angle between the *i*-th receiver and the *j*-th source. ϕ_m is the object rotation angle.

Therefore in the multistatic arrangement shown in Fig. 5(a), the locations of transmitting and receiving antennas can be designed to acquire four lines of Fourier-domain data with equally spacing angles as shown in Fig. 5(b), as k_0 is stepped from $k_{\min}$ to $k_{\max}$. In order to fill the Fourier-domain space, one can then rotate the scattering object to record the scattered field.

A multistatic microwave imaging system is then developed with 1st and 2nd transmitting antennas located at about $0°$ and $-20°$ for simultaneously transmitting frequency-swept microwave signals. The 1st and 2nd receiving antennas are at about $0°$ and $10°$ for collecting the object scattered field. All the transmitting and receiving antennas are in the far-field region. These antennas are connected to a novel four-port test set, an HP8341B synthesized sweeper and an HP8510C network analyzer.

In the measurement, the frequency is stepped from 7.5 to 12.5 GHz for 101 points. The scattering object is sequentially rotated for 18 different angular ranges to synthesize a total of $360°$ Fourier-domain data with $1°$ interval. In other words, one can effectively reduce the object rotation angles by four times using this multistatic arrangement with two transmitting antennas and two receiving antennas.

The measured Fourier-domain data of the metallic cylinder is shown in Fig. 7(a) and the reconstructed images is shown in Fig. 7(b). A complete circle image is shown using multistatic arrangement with $90°$ object rotation angle.

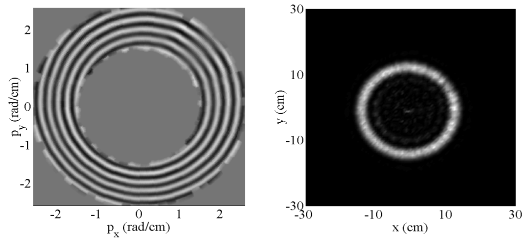

Fig. 6 (a) Measured Fourier-domain data and (b) reconstructed image using multistatic arrangement.

四、結論與討論

In this study, multi-source illumination technique is developed for three frequency-swept microwave imaging systems including quasi-monostatic, bistatic and multistatic arrangements. In each arrangement, the image reconstruction method is developed to extract the corresponding Fourier domain data of the related illumination source from the measured scattered field. These three imaging systems and measurement results demonstrate that the multi-source illumination is an effective approach to enlarge the object Fourier domain, hence to improve the image resolution and object viewing angle.

五、參考論文

[1] N. H. Farhat, "Microwave diversity imaging and automated target identification based on models of neural networks", *Proc. IEEE,* vol.77, pp.670-681, Feb. 1989.

[2] D. B. Lin and T. H. Chu, "Bistatic frequency-swept microwave imaging: principle, methodology and experimental results", *IEEE Trans. Microwave Theory Tech.*, vol.41, pp.855-861, May 1993.

[3] C. H. Tseng and T. H. Chu, "Principle and results of microwave diversity imaging of conducting objects using multisource illumination", *IEE Proc.-Microw. Antennas Propag.,* vol.151, no.2, pp.149-155, April 2004.

[4] C. H. Tseng and T. H. Chu, "Multistatic microwave imaging of perfectly conducting objects," *2004 IEEE AP-S and URSI International Symposium*, Monterey, CA, USA, June 2004.

[5] C. H. Tseng and T. H. Chu, "Improvement of quasi-Monostatic frequency-swept microwave imaging of conducting objects using illumination diversity technique", *IEEE transactions on Antennas and Propagation*, vol.AP-53, no.1, pp.305-312, Jan.2005.